Supplementary Material

Metabolic Consequences of Altered Kidney Glucose Reabsorption under Normoglycemic Conditions

Majdoleen Ahmad[1], Anna Permyakova[1], Saja Baraghithy[1], Nilanjan Sahu[1], Ifat Abramovich[2], Bella Agranovich[2], Ori Shalev[3], Aviram Kogot-Levin[4], Alina Nemirovski[1], Eyal Gottlieb[2], Rinat Abramovitch[5, 6], Gil Leibowitz[4], Liad Hinden[1,*], and Joseph Tam[1,*]

[1]Obesity and Metabolism Laboratory, Institute for Drug Research, School of Pharmacy, Faculty of Medicine, The Hebrew University of Jerusalem, Jerusalem, Israel.

[2]Laura and Isaac Perlmutter Metabolomics Center, B. Rappaport Faculty of Medicine, Technion-Israel Inst of Technology, Haifa, Israel.

[3]Metabolomics Center, Core Research Facility, the Faculty of Medicine, The Hebrew University of Jerusalem, Jerusalem, Israel

[4]Diabetes Unit and Endocrine Service, Hadassah-Hebrew University Medical Center, Jerusalem, Israel.

[5]The Wohl Institute for Translational Medicine, Hadassah-Hebrew University Medical Center, Jerusalem, Israel.

[6]The Goldyne Savad Institute of Gene Therapy, Hadassah-Hebrew University Medical Center, Jerusalem, Israel.

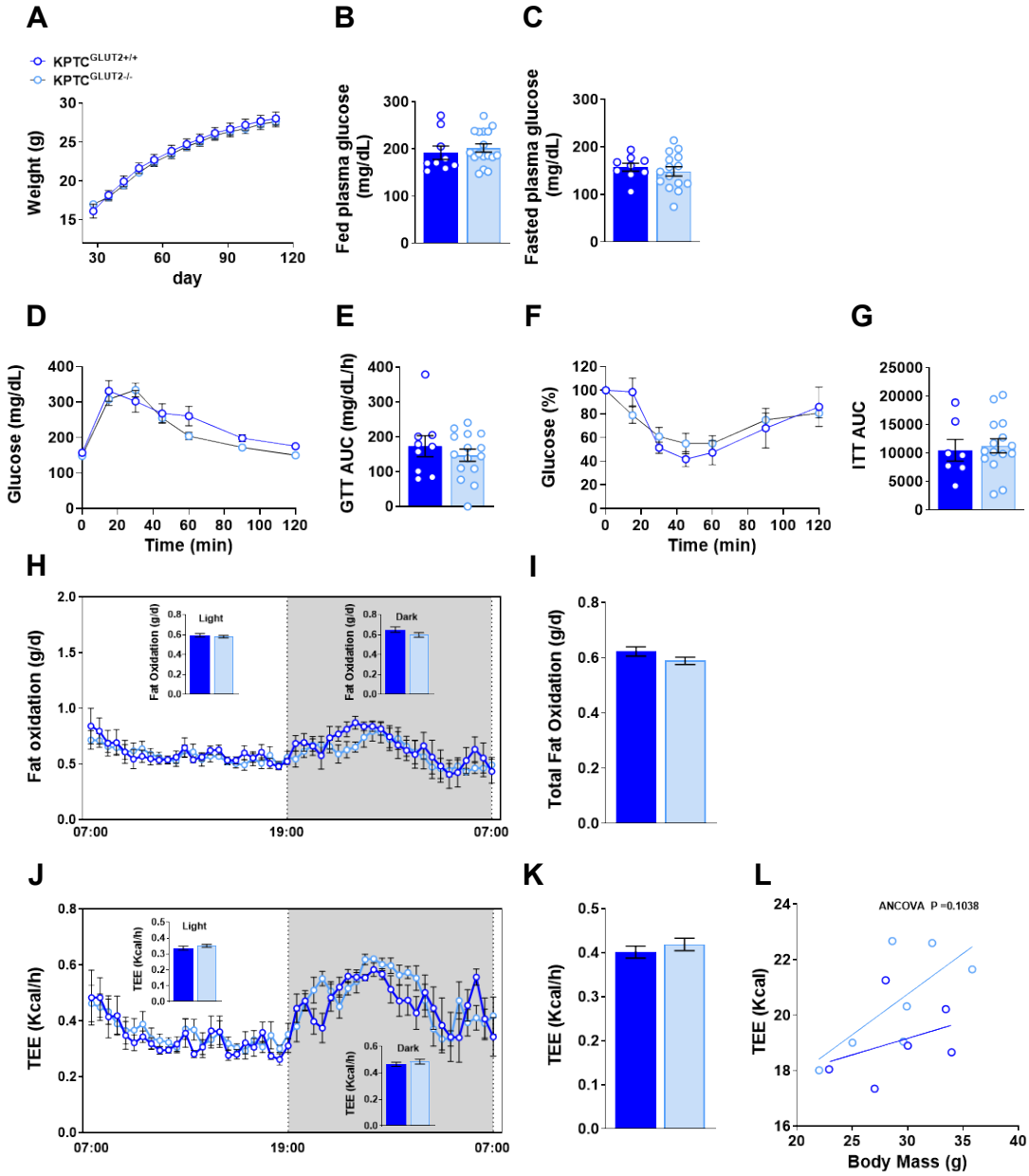

Figure S1. Unchanged glucose homeostasis, fat oxidation and total energy expenditure in KPTC$^{GLUT2-/-}$ mice. 16-weeks-old KPTC$^{GLUT2+/+}$ and KPTC$^{GLUT2-/-}$ mice underwent glucose homeostasis and metabolic assessment. (**A**) No changes were detected in the body weight of the KO mice. Additionally, no significant changes in the (**B**) fed and (**C**) fasting plasma glucose levels, (**D, E**) glucose tolerance and (**F, G**) insulin sensitivity. 24-hours (**H, I**) fat oxidation and (**J, K**) total energy expenditure (TEE) measurements (**L**) and its associated ANCOVA analysis revealed no significant changes. For **A**; KPTC$^{GLUT2+/+}$ n = 16 mice and KPTC$^{GLUT2-/-}$ n = 17 mice. For **B** and **C**; KPTC$^{GLUT2+/+}$ n = 9 mice and KPTC$^{GLUT2-/-}$ n = 17 mice. For **D-G**; KPTC$^{GLUT2+/+}$ n = 7 mice and KPTC$^{GLUT2-/-}$ n = 15 mice. For **H-L**; KPTC$^{GLUT2+/+}$ n = 6 mice and KPTC$^{GLUT2-/-}$ n = 7 mice. Data represent the mean ± SEM and were analyzed by Unpaired Two-tailed Student's t-test. The EE ANCOVA analysis done for this work was provided by the NIDDK Mouse Metabolic Phenotyping Centers (MMPC, www.mmpc.org) using their Energy Expenditure Analysis page (http://www.mmpc.org/shared/regression.aspx) and supported by grants DK076169 and DK115255.

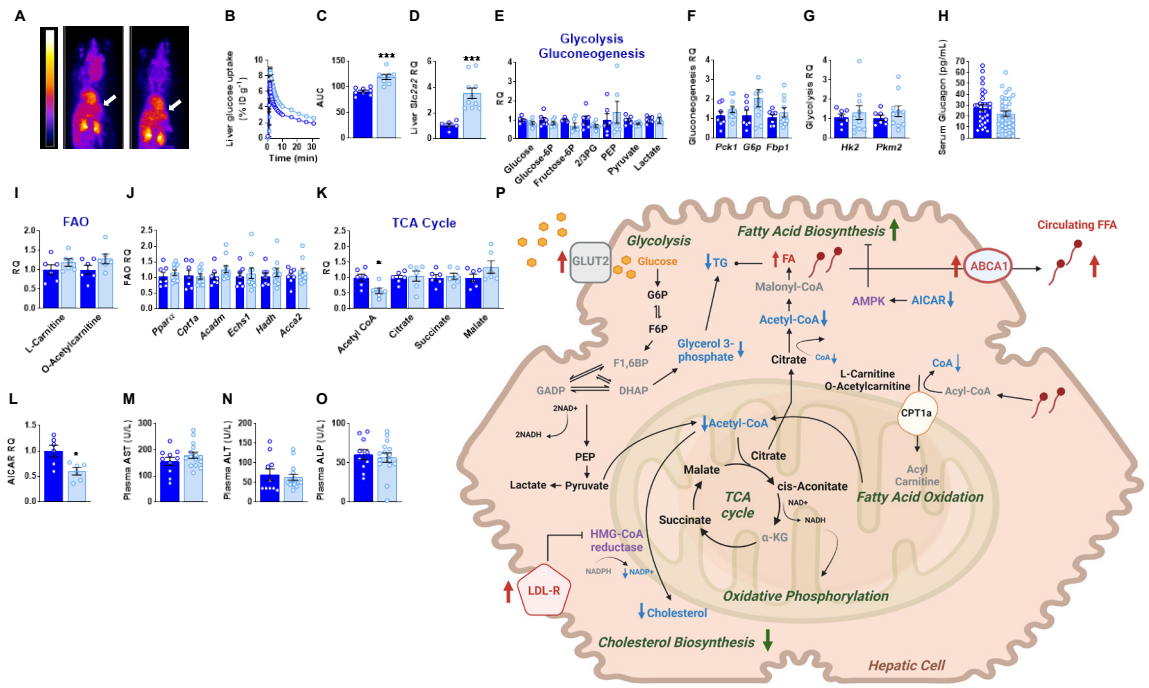

Figure S2. Liver metabolic changes in KPTC$^{GLUT2-/-}$ mice. Glucose uptake assessed using PET-MRI, revealed significant elevation in (**A-C**) liver glucose uptake, corresponding to the (**D**) enhanced liver transcriptional expression of *Slc2a2* (GLUT2), found in liver lysates of KPTC$^{GLUT2-/-}$ mice. However, liver metabolomics analysis shown (**E**) no significant changes in metabolites related to glycolysis and gluconeogenesis nor in (**F, G**) the transcriptional expression levels of main enzymes in these pathways or (**H**) in serum glucagon levels measured using ELISA. Additionally, (**I**) no change was found in metabolites involving FAO using metabolomics analysis, nor in (**J**) the transcriptional expression levels of main enzymes in this pathway. (**K**) No change was found in metabolites involving TCA cycle using metabolomics analysis, except for a significant reduction in Acetyl-CoA. (**L**) A significant decrease in the level of AMPK activator; AICAR was found using metabolomics analysis. Biochemical analysis of plasma liver enzymes revealed no change in (**M**) AST, (**N**) ALT, and (**O**) ALP in KPTC$^{GLUT2-/-}$ mice. (**P**) illustration of the metabolic changes in hepatic cell of KPTC$^{GLUT2-/-}$ mice (black-unchanged metabolites, gray- undetected metabolites, blue- decreased metabolites, red- increased metabolites). Figure created with BioRender.com. For **B, C**; $n = 8$ mice for each group. For **D, F, G, J**; KPTC$^{GLUT2+/+}$ $n = 6$ mice and KPTC$^{GLUT2-/-}$ $n = 10$ mice. For **E, I, K, L**; $n = 6$ mice for each group. For **M**, **N**, **O**; KPTC$^{GLUT2+/+}$ $n = 10$ mice and KPTC$^{GLUT2-/-}$ $n = 15$ mice. Data represent the mean ± SEM and were analyzed by Student's t-test. *P<0.05, relative to KPTC$^{GLUT2+/+}$ mice. AICAR, 5-aminoimidazole-4-carboxamide ribonucleotide; FAO, fatty acid oxidation; AST, Aspartate Aminotransferase; ALT, Alanine transaminase; ALP, Alkaline phosphatase.

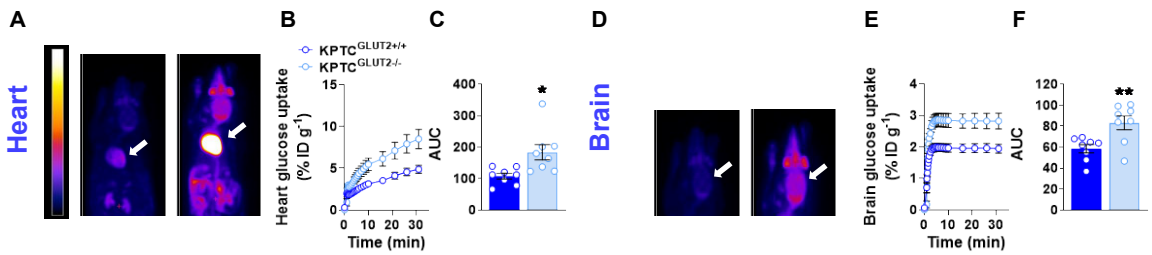

Figure S3. Enhanced heart and brain glucose uptake in KPTC$^{GLUT2-/-}$ mice. Glucose uptake assessed using PET-MRI, revealed a significant increase in (**A-C**) heart and (**D-F**) brain, in KPTC$^{GLUT2-/-}$ mice. For **B, C, E, F**; n = 8 mice for each group. Data represent the mean ± SEM and were analyzed by Student's t-test. *P<0.05, **P<0.005 relative to KPTC$^{GLUT2+/+}$ mice. AUC, area under the curve.

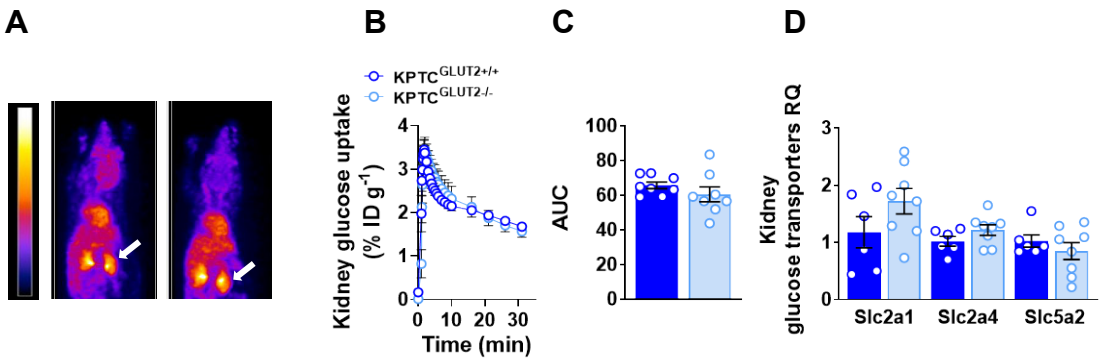

Figure S4. No changes in glucose uptake in the kidney of KPTC$^{GLUT2-/-}$ mice. Glucose uptake assessed using PET-MRI, revealed no significant change in (**A-C**) kidney glucose uptake as well as no (**D**) compensatory elevation in the expression of other GLUT paralogs *Slc2a1* (GLUT1) and *Slc2a5* (GLUT5) or *Slc5a2* (SGLT1) in the kidney of KPTC$^{GLUT2-/-}$ mice. For **B, C**; $n = 8$ mice for each group. For **D**; KPTC$^{GLUT2+/+}$ $n = 6$ mice and KPTC$^{GLUT2-/-}$ $n = 8$ mice. Data represent the mean ± SEM and were analyzed by Student's t-test. AUC, area under the curve.

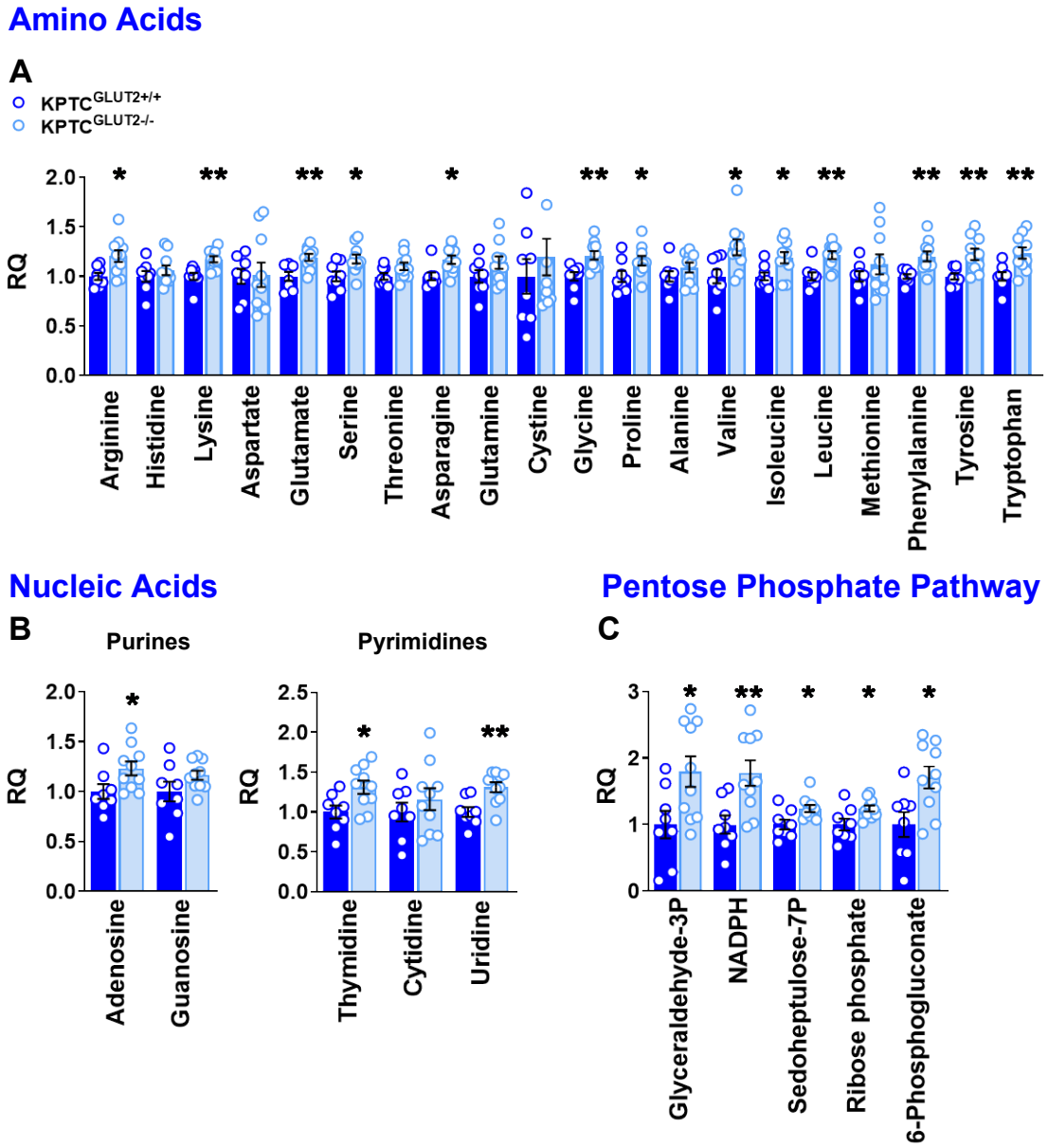

Figure S5. Elevated levels of amino and nucleic acids in KPTC$^{GLUT2-/-}$ mice.
Metabolomics profiling analysis revealed elevated kidney levels of (**A**) multiple amino acids and (**B**) nucleic acids as well as metabolites of the (**C**) pentose phosphate pathway in kidneys extracts from KPTC$^{GLUT2-/-}$ mice (n = 10) compared to those from KPTC$^{GLUT2+/+}$ mice (n = 8). Data represent the mean ± SEM and were analyzed by Unpaired Two-tailed Student's t-test. *P<0.05, **P<0.005 relative to KPTC$^{GLUT2+/+}$ mice.

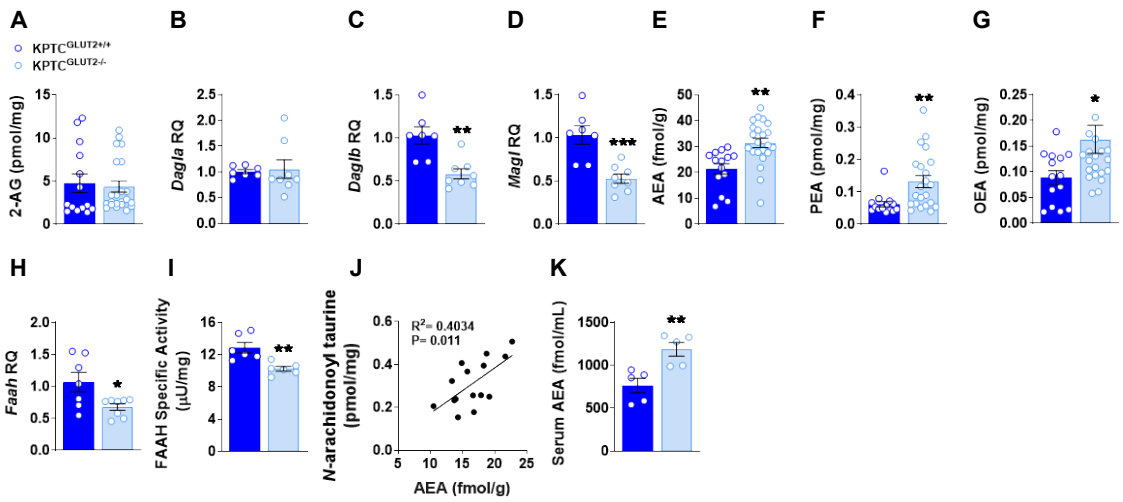

Figure S6. Elevated AEA levels in kidney and serum of KPTC$^{GLUT2-/-}$ mice. (**A**) No changes in kidney 2-AG levels measured using LC-MS/MS, corresponding to the reduced transcriptional levels of its metabolizing enzymes, (**B, C**) *Dagl*α/β and degrading enzymes (**D**) *Magl*. On the other hand, the kidney levels of (**E**) AEA, (**F**) PEA and (**G**) OEA detected using LC-MS/MS, were significantly elevated, corresponding to the transcriptional level of AEA degrading enzymes, (**H**) *Faah* and its (**I**) significantly reduced activity. (**J**) The levels of FAAH substrates; AEA and *N*-arachidonoyl taurine detected using LC-MS/MS, were positively correlated further supporting FAAH inhibition in the kidney of KPTC$^{GLUT2-/-}$ mice. Additionally, (**K**) serum AEA levels were significantly elevated in KPTC$^{GLUT2-/-}$ mice. For **A, E-G**; KPTC$^{GLUT2+/+}$ n = 14 mice and KPTC$^{GLUT2-/-}$ n = 22 mice. For **B-D**, **H**; KPTC$^{GLUT2+/+}$ n = 7 mice and KPTC$^{GLUT2-/-}$ n = 8 mice. For **I**, **K**; n = 6 for each group. For **J**; KPTC$^{GLUT2+/+}$ n = 8 mice and KPTC$^{GLUT2-/-}$ n = 7 mice. Data represent the mean ± SEM and were analyzed by Student's t-test, I was analyzed by one-way ANOVA followed by Tukey's multiple comparison test. *P<0.05, **P<0.005, ***P<0.001, ****P<0.0001 relative to KPTC$^{GLUT2+/+}$ mice or the corresponding control group. 2-AG, 2-arachidonoylglycerol; *Dagl*, diacylglycerol lipase; *Magl*, monoacylglycerol lipase; FAAH, fatty acid amide hydrolase; AEA, *N*-acylethanolamine [anandamide]; PEA, *N*-palmitoylethanolamine; OEA, *N*-oleoylethanolamine.

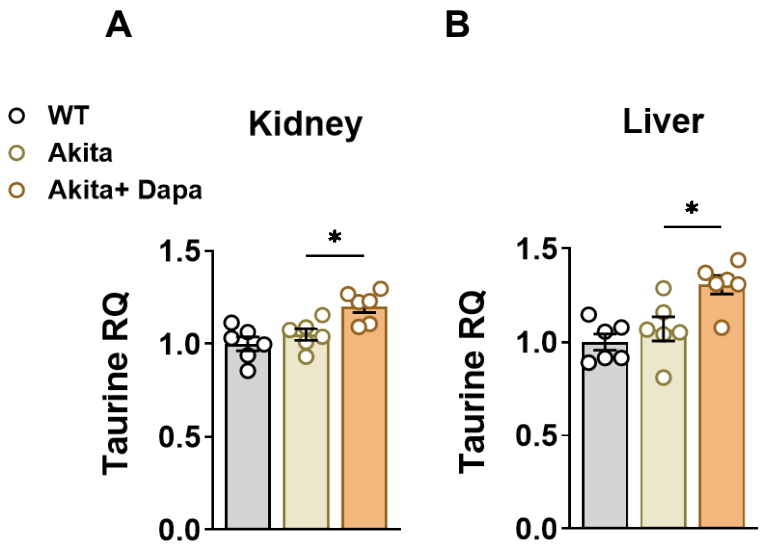

Figure S7. Elevated levels of taurine in diabetic treated with SGLT2i. Metabolomics profiling analysis for taurine in (**A**) kidney and (**B**) liver of diabetic mice treated/untreated with Dapagliflozin. For **A, B**; n = 6 for each group. Data represent the mean ± SEM and were analyzed using One-way ANOVA followed by one-sided Tukey test. *P<0.05 relative to Akita mice.

Table S1. Mouse Primers used for RT-PCR Analysis

Gene	Forward primer (5'-3')	Reverse primer (5'-3')
Acaa2	CAGAGGTGGAAAGCTGCTAA	GCATGGTCTGTTTGCCTTTC
Acadm	CAGCCAATGATGTGTGCTTAC	CATACTCGTCACCCTTCTTCTC
Aldob	CCAGCCTTGCTATCCAAGAA	GCACCTCTGGCTCAACAATA
B2m	ATGGGAAGCCGAACATACTG	CAGTCTCAGTGGGGGTGAAT
Baat	CCTGAGACATCCTAAGGTCCT	TACTGGGTACAGGTGGGTAGA
Cdo	ACTCGGCGGGATTGCTC	ACCCTGGCGGACCTCAT
Cidea	CTTGGGGGTGGTACCCAGTG	ATCCACGCAGTTCCCACACA
Cidec	GCTGAAGGGGCAGAAGTGGA	GCGCTTGGCCTTGTAGCAGT
Cnr1	AAGTCGATCTTAGACGGCCTT	TCCTAATTTGGATGCCATGTCTC
Cpt1a	CCGTGAGGAACTCAAACCTATT	CAGGGATGCGGGAAGTATTG
Csad	CCTGGAGAGGCAGATCATTC	GTCCGTGTCGCTGGCAAAC
Cyp7a1	AACTGGAGCTTGTAGAGAGC	CGTTCAATCATCCAGTGTCC
Dagla	GTCCTGCCAGCTATCTTCCTC	CGTGTGGGTTATAGACCAAGC
Daglb	AGCGACGACTTGGTGTTCC	GCTGAGCAAGACTCCACCG
Echs1	GGACTGTTACTCCAGCAAGTTC	CCCACCAAGAGCATAACCATT
Eno1	CCTAGAACTCCGAGACAATGATAAG	AGAGCAGGCGCAATAGTTT
Faah	GTATCGCCAGTCCGTCATTG	GCCTATACCCTTTTTCATGCCC
Gamt	CACGCACCTGCAAATCCTG	TACCGAAGCCCACTTCCAAGA
Gapdh	CCCTTGAGCTAGGACTGGATAA	GGGCTGCAGTCCGTATTTATAG
Gpam	GCCAGCAAGTCCTGCGCTAT	CCTGCTCGTGTGGGTGATTG
G6p	CCTCGTCTTCAAGTGGATTCTG	GGTGACAGGGAACTGCTTTAT
Hadh	CCAAGAAGGGAATTGAGGAGAG	ACAAACTCATCTCCAGCCTTAG
Hk2	GCTGGAGGTTAAGAGAAGGATG	TGGAGTGGCACACACATAAG
Mgll	ACCATGCTGTGATGCTCTCTG	CAAACGCCTCGGGGATAACC
Mogat1	CCAGCGCAAAGGGTTTGTT	CACCAAAAGAAAATACTGGAACCA
mt-Rnr2	CTAGAAACCCCGAAACCAAA	CCAGCTATCACCAAGCTCGT

Pck1	ATCTCCTTTGGAAGCGGATATG	GGTTAGTTATGCCCAGGATCAG
Pcx	CAAGCAGGTAGGCTATGAGAAC	GGGAATTGACCTCGATGAAGTAG
Pkm2	TCCGGACTGGACTCATCAA	GGATGTTCTCGTCACACTTCTC
Pparα	AGAGCCCCATCTGTCCTCTC	ACTGGTAGTCTGCAAAACCAAA
Slc2a1	CTTCACTGTGGTGTCGCTGT	TTCAAAGAAGGCCACAAAGC
Slc2a4	CTGTGCCATCTTGATGACCGTG	GTTGGAGAAACCAGCGACAGC
Slc2a5	GGCGCTGCAGAACACCAT	AAGGCGTGTCCTATGACGTAGAC
Slc5a2	GTGTACGGATCAGGTCATTGT	CATGGGCAGTAGCTTCAGATAG
Srebp1	GATGTGCGAACTGGACACAG	CATAGGGGGCGTCAAACAG
Tpi1	GCACAGGAAGTACACGAGAAG	CCAGTCACAGAACCTCCATAAA
Ubc	GCCCAGTGTTACCACCAAGA	CCCATCACACCCAAGAACA
Gene	**QuantiTect Primer Assays (Qiagen, Germany)**	
Hmgcr	QT01037848	

Acaa, acetyl-CoA acyltransferase; *Acadm,* acyl-CoA dehydrogenase medium chain; *Aldo*, aldolase fructose-bisphosphate; *B2m,* beta-2 microglobulin; *Baat*, bile acid-CoA: amino acid N-acyltransferase; *Cdo*, cysteine dioxygenase; *Cide,* cell death inducing DFFA like effector; *Cpt*, carnitine palmitoyltransferase; *Csad*, cysteine sulfinic acid decarboxylase; *Cyp7a1*, Cholesterol 7 alpha-hydroxylase; Dagl, diacylglycerol lipase; *Echs*, enoyl-CoA hydratase; *Eno*, enolase; *Faah*, fatty acid amide hydrolase; *Gamt*, guanidinoacetate methyltransferase; *Gapdh*, glyceraldehyde-3-phosphate dehydrogenase; *Gpam,* glycerol-3-phosphate acyltransferase, mitochondrial; *G6p*, glucose-6-phosphatase; *Hadh*, hydroxyacyl-CoA dehydrogenase; *Hk,* hexokinase; *Mgll,* monoglyceride lipase; *Mogat,* monoacylglycerol O-acyltransferase; *mt-Rnr2,* 16S rRNA, mitochondrial; *Pck*, phosphoenolpyruvate carboxykinase; *Pcx*, pyruvate carboxylase; *Pkm,* pyruvate kinase M*; Ppar,* peroxisome proliferator activated receptor; *Slc*, solute carrier family; *Srebp*, Sterol regulatory element-binding proteins; *Tpi*, triosephosphate isomerase; *Ubc*, ubiquitin C; *Hmgcr*, 3-hydroxy-3-methyl-glutaryl-coenzyme A reductase.

Table S2. MRM transitions ion modes.

Compounds	Precursor ion (m/z)	Ionization ESI (-)	Fragment (m/z)	DP (volts)	CE (volts)
NAT	410.2	$[M-H]^-$	107.0	-85	-44
d_4-NAT	414.2	$[M-H]^-$	109.9	-85	-44
Compounds	**Precursor ion (m/z)**	**Ionization ESI (+/-)**	**Fragment (m/z)**	**DP (volts)**	**CE (volts)**
Taurine	124	$[M-H]^-$	80	20	12
Creatine	132	$[M+H]^+$	44	35	40
S-(2-Aminoethyl)-L-cysteine	165	$[M+H]^+$	120	16	14

NAT, *N*-arachidonoyl taurine.